Sound emission from jets at high subsonic velocities

By ERIK MOLLÖ-CHRISTENSEN
AND RODDAM NARASIMHA
Department of Aeronautics and Astronautics, Massachusetts Institute of Technology

(Received 16 September 1959)

Measurements of spectra of sound emission to the far field from jets at high subsonic velocities are presented. The similarity relations found in the experiments suggest a mechanism of sound generation and scattering where the latter is of dominant importance. A possible mechanism is described.

1. Introduction

This paper reports on some measurements performed at the California Institute of Technology during the past year. While many results of jet noise measurements were available in the literature, no single set of experiments was sufficiently complete to allow one to establish the similarity relations for the spectra of emitted sound.

The purpose of our experiments was to find these similarity relations. This can be attained only by performing the experiments under closely controlled circumstances which are difficult to obtain, as was soon discovered. Parasitic variables, involving the amplitude of sound from the air supply, the reflectivity of the surroundings and scattering from the microphone all presented serious problems. Only after months of attention to these details was it possible to obtain meaningful narrow band-pass data, which would yield the spectral definition required.

2. The air flow arrangement

The experimental arrangement is shown in figure 1. From the laboratory air supply the air passed through a water separator, a reducing valve and a throttling valve through a flexible hose to the settling chamber. The settling chamber was lined with 1 in. fibreglass mats, and contained twelve perforated disks, made up from plywood faced on both sides with fibreglass. The perforations consisted of eight 1 in. holes randomly arranged. The baffles were followed by three screens. The first contraction was made of plaster of Paris, and after a short straight run through a 2 in. smooth pipe, the air entered the final nozzle. The nozzles were made of brass, polished on the inside; they all ended in a straight run, three diameters long for each of two 'laminar' nozzles 0·375 and 0·201 in. diameter, and about forty-three diameters long for the turbulent nozzle, 0·375 in. diameter. The overall contraction ratio, based on area, varied from approximately 100 to 400.

The anechoic chamber, in which all the measurements were performed, was 8×8 ft. in cross-section, and was 10 ft. long. Its anechoic properties were judged

to be satisfactory after the jet noise measurements showed the existence of far-field similarity of spectra, within experimental accuracy. No far field can exist inside a reflecting enclosure.

Measurement of the sound level at the end of the first contraction at maximum mass flow showed it to have a root-mean-square amplitude of less than 1 dyne/cm^2;

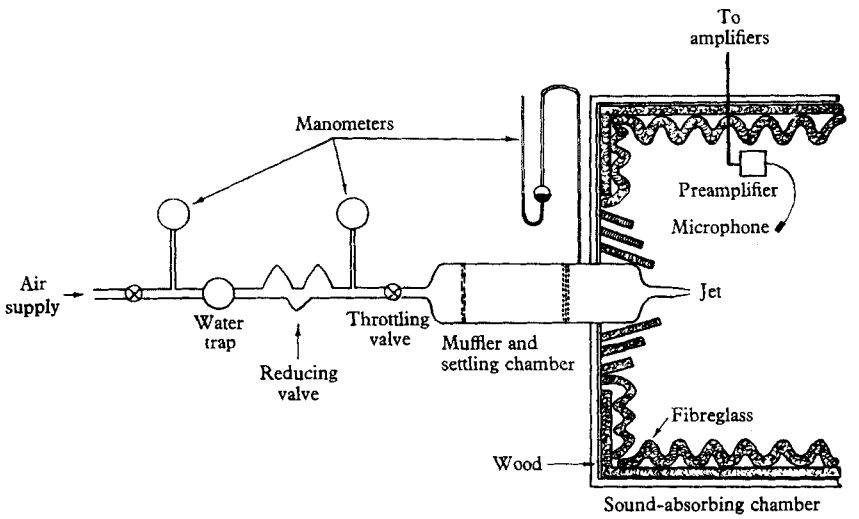

FIGURE 1. Experimental arrangement.

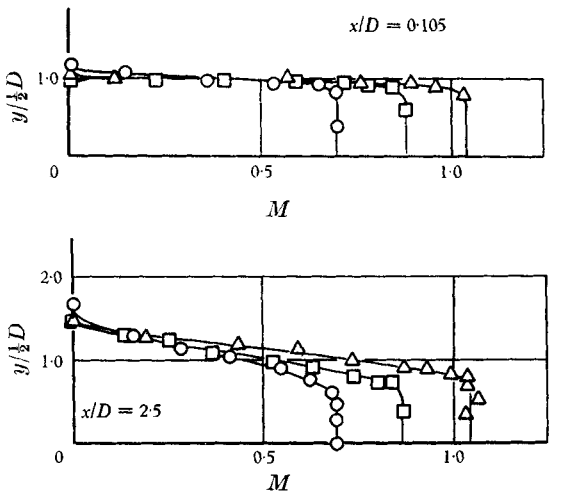

FIGURE 2. Mach number profiles for 0·201 in. diameter jet. ○, $M = 0{\cdot}70$; □, $M = 0{\cdot}88$; △, $M = 1{\cdot}04$.

most of this noise was outside the frequency band of the measurements. The use of small capillary tubing for transmitting the pressure in the stagnation chamber to the manometer effectively prevented cavity resonance in this tube.

Profiles of the Mach numbers of the resulting flow are shown in figures 2, 3 and 4 for several jet Mach numbers.

3. Method of sound measurement and recording

A barium titanate microphone of the type designed by Willmarth (1958) was used in all the measurements. The face diameter of the microphone was 0·25 in. A small shock tube was built and used for microphone calibration.

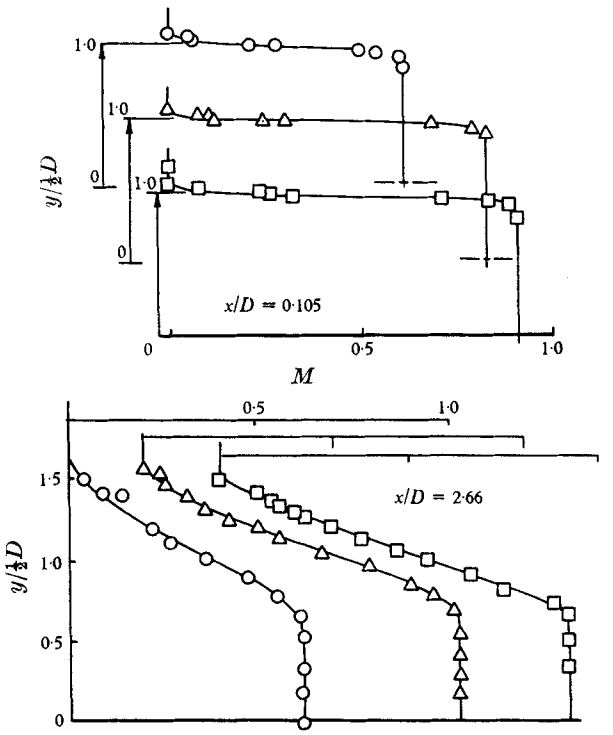

FIGURE 3. Mach number profiles for 0·375 in. diameter jet. ○, M = 0·61; △, M = 0·83; □, M = 0·91.

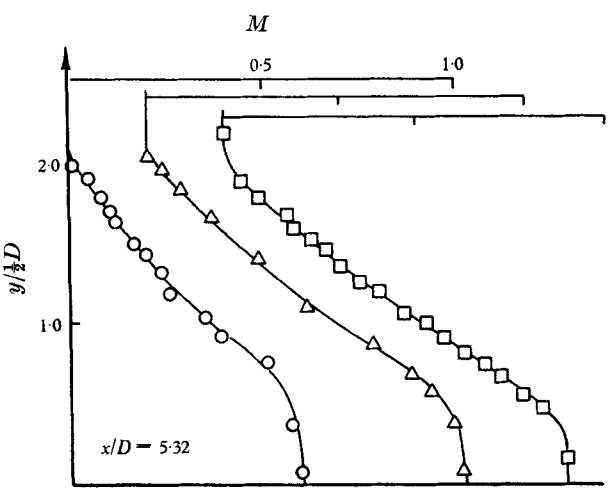

FIGURE 4. Mach number profiles for 0·375 in. diameter jet. ○, M = 0·61; △, M = 0·83; □, M = 0·91.

The amplifiers designed and built for the purpose gave a r.m.s. noise level of 1·7 mV at the input, or, in terms of pressure, 1 dyne/cm^2, over the band-width 500 c/s to 100 kc/s.

The signal from the amplifier was passed through a band-pass filter, cutting off at 500 and 100,000 c/s. The signal then went into a true r.m.s. meter, into an oscilloscope for monitoring against overloads and a Donner Model-21 wave-form analyser. The output from the wave-form analyser went to a low-pass filter, for averaging, and the filter output was recorded by a pen recorder.

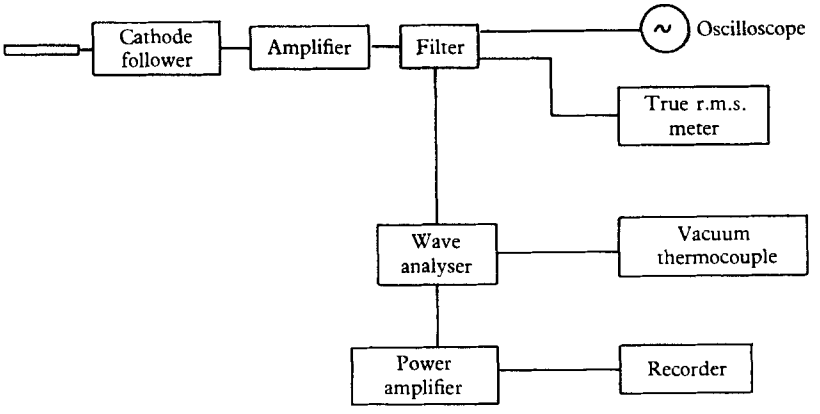

FIGURE 5. Block diagram of recording equipment.

The power band-width (Q_p) of the wave-form analyser was 45 c/s, a measure of the width of an equivalent rectangular spectral window.

The frequency dial of the wave-form analyser was driven by a clockmotor, and its position recorded by the other pen of the pen recorder. Taking account of the traversing speed of the frequency dial, the resulting spectra were thus averaged over a maximum of three band-widths.

In addition to this primary equipment, many pieces of secondary equipment were used from time to time in the development of a satisfactory experimental arrangement.

The microphone was supported on a thin wire, and was pointed at the jet nozzle to minimize scattering. In spite of this, scattering occurred at approximately 37,000 c/s, as could be seen in the spectra. No data were taken above this frequency.

A block diagram of the recording system is shown in figure 5.

4. Dimensional analysis and similarity of emitted sound

In the study of aerodynamically generated sound, the fluctuating pressure $p'(\mathbf{r}, t)$ is measured. Its statistical properties determine the structure of the sound field and its relation to the sound-producing flow.

The simplest and most important quantities to be measured are the mean square pressure $\overline{p'^2}$ and the power spectral density $\phi(f, \mathbf{r})$ with respect to frequency f (c/s). They are related by $\overline{p'^2} = \int \phi \, df$.

The sound-producing flow is described by a set of parameters which involve at least the following: density ρ, kinematic viscosity ν, velocity of sound a, velocity U and a characteristic length D. There will also be a number of other parasitic parameters, such as the sound and turbulence levels of the stream used, the microphone diameter, the cut-off frequencies of the recording equipment, the averaging time, etc.

Indeed, the decisive part of an experimental study of aerodynamic noise lies in the identification and elimination of parasitic parameters. This is obvious for any experiment; it is emphasized here for the case of aerodynamic noise because the nature of the problem, namely, the study of a random wave-field of small intensity without *a priori* knowledge of what to expect, often makes it very difficult to know whether one has succeeded in measuring what was intended or not.

If one assumes that all parasitic parameters have been eliminated, dimensional analysis yields for the form of $\overline{p'^2}$ and ϕ

$$\overline{p'^2} = \rho^2 U^4 F\left(\frac{\mathbf{r}}{D}, Re, M\right),$$

where $Re = UD/\nu$ and $M = U/a$ are Reynolds number and Mach number, respectively; and

$$\phi(f, \mathbf{r}) = \rho^2 U^4 \frac{D}{V} G\left(\frac{\mathbf{r}}{D}, \frac{fD}{V}, Re, M\right),$$

where V is some characteristic velocity.

If one adds some physical insight to the process of dimensional analysis, one may find that only certain combinations of the dimensionless variables occur. For example, one may apply the law of conservation of radiated energy in the far field of an emitter of limited size, from which one finds that the intensity must fall off as $1/r^2$. Thus,

$$\overline{p'^2} = \rho^2 U^4 \frac{D^2}{r^2} F_1(\theta; Re, M),$$

$$\phi = \rho^2 U^4 \frac{D^3}{Vr^2} G_1\left(\theta, \frac{fD}{V}; Re, M\right),$$

where r is the distance from the jet exit and θ the angle $\mathbf{r}$ makes with the jet axis.

To go beyond this stage, one must adopt a more detailed physical model. The choice of physical models will be suggested by the results of the experiments, this being a purpose of experiment.

From these similarity considerations it was decided to present the results in the following form, with $V = a = a_0$,

$$g\left(\frac{fD}{a}, Re, M, \theta\right) = \left\{\frac{r^2}{D^2} \frac{1}{p_A^2 M^4} \frac{a}{D} \frac{Re^n}{M^m} \phi\left(\frac{fD}{a}, r, \theta, Re, M\right)\right\}^{\frac{1}{2}}.$$

The reasons for the different terms are the following.

r^2/D^2 takes account of the far-field radiation law.

$\frac{1}{p_A^2 M^4} \sim \frac{1}{\rho^2 U^4}$ scales the pressure fluctuation by the jet dynamic pressure, or, alternatively, the spectral intensity or spectral sound energy flux through the jet nozzle, $\frac{1}{2}\rho U^3$ times the Mach number.

a/D establishes the time constant.

Re^n/M^m is a multiplying factor; the exponents are chosen such as to enable all the data to be plotted as closely on a single curve as possible.

5. Measured sound spectra

The measured far-field spectra are shown in figures 6–10. In each case, the similarity parameter Re^n/M^m was chosen such as to give the best possible fit. The spectra have been plotted on linear scales, as it was thought that this would be more revealing than the usual octave-decibel system.

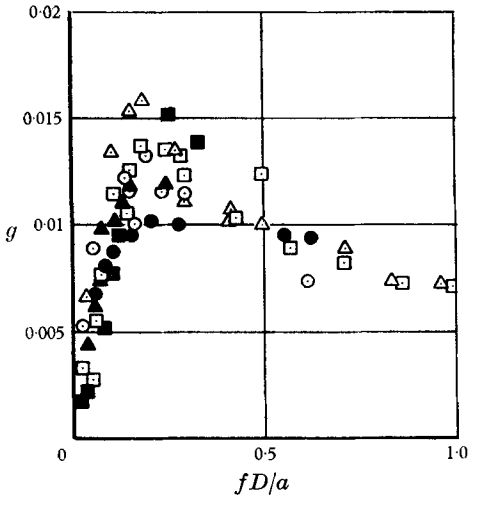

FIGURE 6. Similarity in spectra at $r = 20{\cdot}5$ in. and $\theta = 25°$.

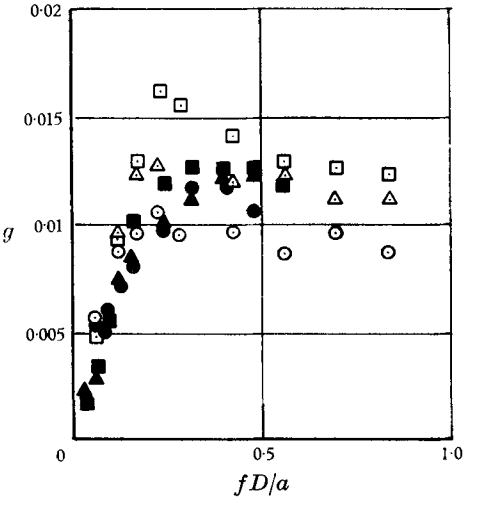

FIGURE 7. Similarity in spectra at $r = 20{\cdot}5$ in. and $\theta = 35°$.

In figures 6–10 the following notation is used:

$$g = \left[\frac{r^2}{D^2}\frac{a}{Q_p D}\frac{\overline{p'^2}}{p_A^2}\frac{1}{M^{4+m}}\frac{R}{R_{\text{ref.}}}\right]^{\frac{1}{2}},$$

M	$D = 0{\cdot}375$ in.	$D = 0{\cdot}201$ in.
0·70	⊙	●
0·88	△	▲
0·99	⊡	■

(Here $\overline{p'^2}/Q_p$ denotes power spectral density, $\overline{p'^2}$ being the mean-square pressure within the bandpass Q_p of the wave analyser.)

In figures 6 and 7, $m = 6$.

Some of the spread in the data is probably due to experimental inaccuracy, and some of it due to application of an inexact similarity parameter. For example, it should not be expected that for the entire spectrum at any given point there would be *no* relation between M and fD/a in the function g.

Considering the spectra as they have been presented, a few features are immediately apparent.

(1) Reynolds number appears to be an important similarity parameter as far as sound emission is concerned.

(2) In most regions, the spectra scale slightly better with fD/a than with fD/U.

(3) Spectra near the jet show a maximum intensity at a Strouhal number $fD/a = 0{\cdot}2$, but for $\theta = 35°$ there was no maximum in the frequency band in which measurements were made.

(4) The power of Mach number which gives the best similarity varies with θ from $m = 4$ at $\theta = 90°$ and $m = 6$ at 25°.

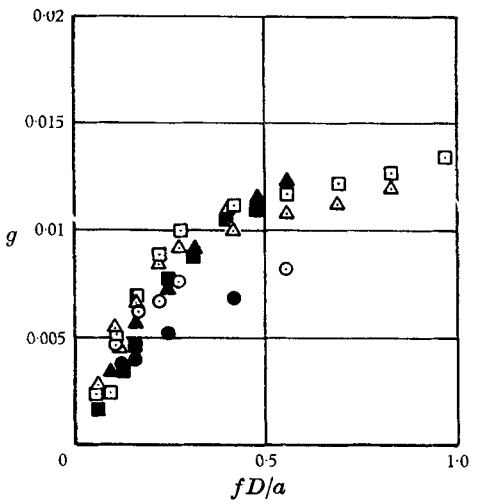

FIGURE 8. Similarity in spectra at $r = 20{\cdot}5$ in. and $\theta = 45°$. See figure 6 for notation; $m = 6$.

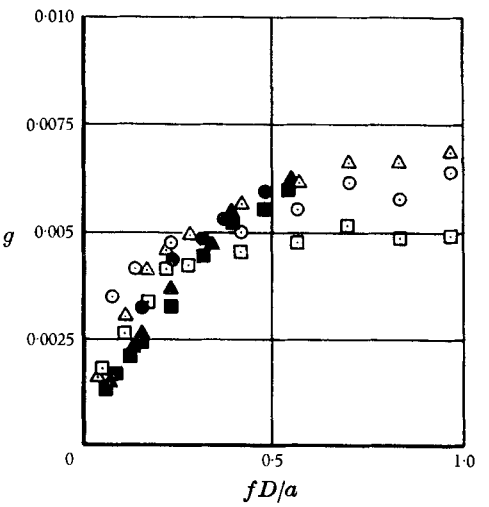

FIGURE 9. Similarity in spectra at $r = 20{\cdot}5$ in. and $\theta = 60°$. See figure 6 for notation; $m = 5$.

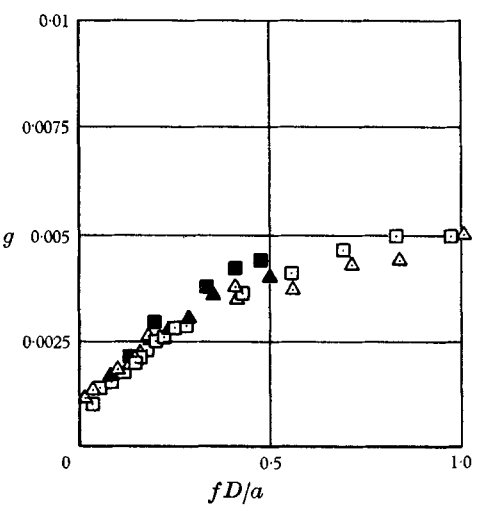

FIGURE 10. Similarity in spectra at $r = 20{\cdot}5$ in. and $\theta = 90°$. See figure 6 for notation; $m = 4$.

6. Outline of a working hypothesis of jet noise

The appearance of Reynolds number as a similarity parameter in the far-field noise suggests that the far-field noise is generated in a region of the jet where Reynolds number is an important parameter. The only such region is the region

of high mean shear immediately downstream of the nozzle. Here the thickness of the shear layer is determined by the thickness of the boundary layer on the nozzle wall at the exit, and this boundary-layer thickness depends strongly upon Reynolds number.

It appears that all the features of the observed far-field spectra can be explained in terms of a generator of sound in the early free-shear layer, and scattering of this sound by the mean flow of the jet. As will be shown, this scatter is coherent for long wavelengths, and partly omnidirectional for short wavelengths. The scatter is thus to some extent frequency selective; the most striking consequence of this is the appearance of a maximum at low frequencies in the spectra near the jet axis.

As will be discussed later, the sound emission from the early shear layer will be that of a dipole sheet, probably anticorrelated about a diameter. Further downstream, turbulence increases, and the turbulent sound sources in the turbulent mixing region possess space correlations of much higher order than the sound sources in the early shear layer, and therefore the radiation to the far field is negligible in comparison. In the near field, these pressure fluctuations with high-order correlation may be dominant, but they will radiate very little energy to the far field.

The lowest order sound emitter has thus been located. We proceed to examine the scattering of sound from the early shear layer by the flow in the jet. For sound of wavelengths of several jet diameters, such that the wavelength is large compared to the mean shear layer thickness, the scattering may be approximated by that of a discrete shear layer with uniform flow inside and still air outside. A sound wave travelling in the downstream direction will be moving with the velocity of sound with respect to the air in the jet, and with a Mach number of $M+1$ with respect to the air outside. The transmitted radiation will therefore be predominantly in the direction $\theta = \cos^{-1}[1/(1+M)]$. A sound wave moving obliquely to the jet axis will be transmitted and reflected from the shear layer. The reflected wave will be different in phase from the impinging wave (Ribner 1957) so that certain wavelengths longer than two jet diameters will resonate back and forth across the jet. This will cause an increase in the radiation of such wavelengths to angles of $\theta = \cos^{-1}[1/(1+M)]$. However, the waves which have bounced back and forth many times will by then have been carried far downstream into the fully turbulent region of the jet, where the mean Mach number has decreased, and will therefore be radiated to points nearer the jet axis than $\theta = \cos^{-1}[1/(1+M)]$.

This accounts for the low-frequency maximum in the spectra near the jet axis. The wavelength which gives maximum resonance across the jet appears to correspond to $fD/a \doteqdot 0{\cdot}2$, as can be seen from the measured spectra.

For shorter wavelengths the scales of turbulence must be considered in the scattering phenomenon. In addition to direct transmission of the primary wave to regions in the vicinity of $\theta = \cos^{-1}[1/(1+M)]$ as before, the waves of wavelength comparable with the scale of turbulence will experience a more or less omnidirectional scattering, and this omnidirectional scattering will be most intense for the very short wavelengths, which will be scattered omnidirectionally

from the early part of the mixing region, where turbulence is most intense. This high-frequency omnidirectional radiation is apparent in the spectra. In addition to the scattered radiation, there is direct outward radiation from the early shear layer. This direct outward radiation will be of dipole character, and the dipoles will probably move at half the jet velocity. The angular intensity distribution of this radiation will be as $\sin\theta/(1-\frac{1}{2}M\cos\theta)^2$.

It is, of course, possible to replace both the sound generation and scattering mechanisms by a source distribution on the jet axis and obtain a correct representation of the far field. The separation of sound generation and coherent and omnidirectional scattering of the sound emitted by the generators chosen here does have the advantage of being closer to the physical processes which cause the noise observed in the far field.

In general, this model gives results in qualitative agreement with experiment. In particular, it gives an explanation of the maximum at low frequencies observed in the spectra near the jet axis, which other models of jet noise have failed to do.

7. Similarity laws for noise generation in the high shear region

These similarity laws are best obtained by rewriting the equations of motion of a gas as a non-homogeneous wave equation, as Lighthill (1952) has done. From the continuity equation

$$\frac{\partial\rho}{\partial t}+\frac{\partial}{\partial x_i}(\rho v_i)=0 \tag{7.1}$$

and the momentum equation

$$\frac{\partial(\rho v_i)}{\partial t}+\frac{\partial}{\partial x_j}(\rho v_i v_j)=-\frac{\partial p}{\partial x_i}+\frac{\partial}{\partial x_j}\tau_{ij} \tag{7.2}$$

one obtains, by adding the divergence of (7.2) to $a_0^2\nabla^2\rho$ and using (7.1)

$$-\frac{\partial^2\rho}{\partial t^2}+a_0^2\nabla^2\rho=-\frac{\partial^2}{\partial x_i\partial x_j}(\rho v_i v_j-\tau_{ij})-\nabla^2(p-a_0^2\rho). \tag{7.3}$$

Assuming a perfect gas and making use of the relations

$$\left(\frac{\partial p}{\partial\rho}\right)_S=a^2=\gamma RT;\quad \left(\frac{\partial p}{\partial S}\right)_\rho=\frac{p}{c_p}$$

one may derive

$$\begin{aligned}-\frac{\partial^2\rho}{\partial t^2}+a_0^2\nabla^2\rho=&-\frac{\partial^2}{\partial x_i\partial x_j}(\rho v_i v_j-\tau_{ij})+(a_0^2-a^2)\nabla^2\rho\\&-\left\{+\frac{p}{c_p}\nabla^2 S+\gamma R\frac{\partial\rho}{\partial x_i}\frac{\partial T}{\partial x_i}+\frac{1}{c_p}\frac{\partial S}{\partial x_i}\frac{\partial p}{\partial x_i}\right\}.\end{aligned} \tag{7.4}$$

This, with some minor modifications, is the equation used by Lighthill. For low Mach numbers the right-hand side can, as a first approximation, be considered known and so treated as a source term. At higher Mach numbers, however, scattering and convection cannot be neglected, and the right-hand side would contain terms depending on the sound emitted, a physical emitter being by its nature also a scatterer.

Chu & Kovasznay (1958) have considered the conditions under which Lighthill's approximation is valid. The sufficient conditions they find restrict, in principle, the approximation to weak turbulence in almost uniform flow.

In the presence of large gradients in the mean flow it is advantageous to write each variable as the sum of its time average and a fluctuation about this average. Denoting them by a bar and prime, respectively, (7.4) becomes

$$-\frac{\partial^2\rho'}{\partial t^2}+a_0^2\nabla^2\rho' = -\frac{\partial^2}{\partial x_i\partial x_j}(\overline{\rho v_i}v_j'+\overline{\rho v_j}v_i'+\rho'\overline{v_iv_j} +\rho'v_i'\overline{v_j}+\bar{\rho}v_i'v_j'+\rho'\overline{v_i}v_j'+\rho'v_i'v_j'-\tau_{ij}') -\left\{\gamma R\left(\frac{\partial\bar{\rho}}{\partial x_i}\frac{\partial T'}{\partial x_i}+\frac{\partial\rho'}{\partial x_i}\frac{\partial\bar{T}}{\partial x_i}\right)+\frac{\bar{p}}{c_p}\nabla^2S' +\frac{p'}{c_p}\nabla^2\bar{S}+\frac{1}{c_p}\left(\frac{\partial\bar{S}}{\partial x_i}\frac{\partial p'}{\partial x_i}+\frac{\partial S'}{\partial x_i}\frac{\partial\bar{p}}{\partial x_i}\right)\right\}, \tag{7.5}$$

where the steady terms on both sides have been cancelled and second-order terms in ρ', T' and S' have been neglected.

Now restrict the discussion to the flow near the nozzle where there is a very thin shear layer separating the uniform parallel flow from the quiescent air outside the jet. If n is distance measured normal to the shear layer, the gradient $\partial\overline{v_1}/\partial n$ is very large, and so the dominant terms on the right-hand side are the ones that involve this derivative. Neglecting entropy and temperature gradients in the flow, we get from (7.5)

$$-\frac{\partial^2\rho'}{\partial t^2}+a_0^2\nabla^2\rho'-\overline{v_1^2}\frac{\partial^2\rho'}{\partial x_1^2}-\frac{2\overline{\rho v_1}}{\bar{\rho}}\frac{\partial^2\rho'}{\partial x_1\partial t}\simeq -2\frac{\partial\overline{\rho v_1}}{\partial n}\frac{\partial v_n'}{\partial x_1} \tag{7.6}$$

for the field inside the jet, and

$$-\frac{\partial^2\rho'}{\partial t^2}+a_0^2\nabla^2\rho'\simeq -2\frac{\partial\overline{\rho v_1}}{\partial n}\frac{\partial v_n'}{\partial x_1} \tag{7.7}$$

outside the jet, the right-hand side being zero outside the jet in both cases.

Equations (7.6) and (7.7) show that the shear layer acts like a dipole-sheet emitter. The strength of the dipoles is not known *a priori*, but their total strength at any instant has to be zero if the efflux from the jet is steady. The net effect is that the shear layer will appear from the outside as a longitudinal-lateral quadrupole.

If the right-hand side in (7.7) *is* considered known, we can formally write down for the density fluctuation in the far field (as in (4))

$$\rho'(\mathbf{x},t)=-\frac{1}{2\pi a_0^3}\underset{\text{dipole volume}}{\iiint}\frac{\partial(\overline{\rho v_1(\mathbf{y})})}{\partial n}\frac{(y_1-x_1)}{|\mathbf{y}-\mathbf{x}|^2}\frac{\partial}{\partial t}\left\{v_n'\left(\mathbf{y},t-\frac{|\mathbf{x}-\mathbf{y}|}{a_0}\right)\right\}dV_{\mathbf{y}}.$$

We can now find the similarity law as follows. The analysis is admittedly rather crude, and is really justified only by the agreement of the final results with experiment. If δ is the shear-layer thickness, we now assume that the thickness and length of the dipole region are each proportional to δ, also that

$$\partial\overline{\rho v_1}/\partial n\sim(\bar{\rho}U/\delta)\quad\text{and}\quad v_n'\sim U.$$

We also assume that the characteristic time of the fluctuations varies like D/U, so that

$$\partial v_n'/\partial t \sim U^2/D.$$

The peripheral distance around the sheet is proportional to D, so we get

$$\rho' \sim \frac{1}{a_0^3 r}\frac{\bar{\rho}U}{\delta}\frac{U^2}{D}D\delta^2 \sim \bar{\rho}M^3\frac{D}{r}\frac{\delta}{D}.$$

For geometrically similar nozzles we might take $\frac{D}{\delta} \sim \sqrt{\frac{UD}{\nu}} = \sqrt{Re}$, so that one finally obtains

$$\frac{\rho'}{\bar{\rho}} \sim M^3\frac{D}{r}\frac{1}{\sqrt{\mathrm{Re}}}.$$

This yields

$$\frac{\overline{p'^2}}{\bar{p}^2} \sim \frac{M^6}{Re}\left(\frac{D}{r}\right)^2$$

and shows the experimentally found dependence on Reynolds number. The power of the Mach number was in most cases somewhat higher, presumably due to the effects of scattering. The spectral density of p' is found to be

$$\phi\left(\frac{fD}{a}, r, \theta, M, Re\right) \sim \frac{D^3}{r^2 a_0}\overline{p'^2}\frac{M^6}{Re}G\left(\frac{fD}{a_0}, \theta\right).$$

8. Jets with turbulent flow at the nozzle exit

From the present understanding of the experimental results, one is strongly led to believe that the mechanism of sound emission to the far field from jets with turbulent flow in the nozzle is the same as that described above.

The spectra obtained with the turbulent pipe flow nozzle, in general, resembled those obtained with the shorter nozzles. A strict comparison between them is not very revealing on account of the very different Mach number profiles for the different nozzles.

9. Conclusions

From a consideration of the similarity relations obtained from experiments, it has been possible to outline a theory of noise emission from subsonic and low supersonic jets.

The sound is generated in the high shear region of the jet, the shear layer of which is considered a dipole sheet with the dipoles oriented along the jet axis. This radiation is emitted both outward and inward. The inwardly emitted radiation is subject to multiple scattering before emergence from the jet. One effect of scattering is the occurrence of a low-frequency peak in the spectrum of emitted sound at an oblique angle to the jet axis, another effect is the increase of energy radiated to $\theta = \cos^{-1}[1/(1+M)]$.

With this description of the mechanism for jet noise, some methods of silencing of jets suggest themselves. It would be beyond the scope of the present paper to discuss them. The apparently intimate connexion between jet stability and noise generation appears worthy of further investigation, as does the effect of sound scattering upon the mean flow in the jet.

The authors have benefited greatly from the experience and advice of Willmarth (1959) and Weyers (1959) in the design of experimental equipment. Also, the frequent discussions with H. W. Liepmann on both theory and experiment are gratefully acknowledged. The amplifiers used in the experiments were built by Richard Swartley. This work was partly supported by the NASA.

REFERENCES

CHU, B-T. & KOVASZNAY, L. S. G. 1958 Non-linear interactions in a heat-conducting compressible gas. *J. Fluid Mech.* **3**, 494.

LIGHTHILL, M. J. 1951 On sound generated aerodynamically. I. General theory. *Proc. Roy. Soc.* A, **211**, 564.

RIBNER, H. S. 1959 Reflection, transmission and amplification of sound by a moving medium. *J. Acoust. Soc. America*, **29**, 431.

WEYERS, PAUL F. R. 1959 The vibration and acoustic radiation of thin-walled cylinders caused by internal turbulent flow. *NASA Memo.* (to be published).

WILLMARTH, W. W. 1958 Small barium titanate transducer for aerodynamic or acoustic pressure measurements. *Rev. Sci. Instrum.* **29**, 218.

WILLMARTH, W. W. 1959 Space-time correlations and spectra of the wall pressure in a turbulent boundary layer. *NASA Memo.* no. 3–17–59 W.